JVI Journals.ASM.org

Structure of a Dengue Virus Envelope Protein Late-Stage Fusion Intermediate

Daryl E. Klein,[a,b] Jason L. Choi,[a] Stephen C. Harrison[a,b,c]

Jack and Eileen Connors Structural Biology Laboratory, Department of Biological Chemistry and Molecular Pharmacology, Harvard Medical School, Boston, Massachusetts, USA[a]; Laboratory of Molecular Medicine, Children's Hospital, Boston, Massachusetts, USA[b]; Howard Hughes Medical Institute, Harvard Medical School, Boston, Massachusetts, USA[c]

The final stages of dengue virus fusion are thought to occur when the membrane-proximal stem drives the transmembrane anchor of the viral envelope protein (E) toward the fusion loop, buried in the target cell membrane. Crystal structures of E have lacked this essential stem region. We expressed and crystallized soluble mutant forms of the dengue virus envelope protein (sE) that include portions of the juxtamembrane stem. Their structures represent late-stage fusion intermediates. The proximal part of the stem has both intra- and intermolecular interactions, so the chain "zips up" along the trimer seam. The penultimate interaction we detected involves the conserved residue F402, which has hydrophobic contacts with a conserved surface on domain II. These interactions do not require any larger-scale changes in trimer packing. The techniques for expression and crystallization of sE containing stem reported here may allow further characterization of the final stages of flavivirus fusion.

The membrane-spanning envelope glycoprotein protein (E) of flaviviruses is both the principal determinant of icosahedral virion assembly and the fusion catalyst for merging viral and target cell membranes (Fig. 1) (1, 2). The E protein folds into three domains, a membrane-proximal stem, and a transmembrane anchor (Fig. 1A). Various crystal structures have shown the arrangement of the three folded domains in both a dimeric prefusion conformation (Fig. 1C) (3, 6) and a low-pH-induced postfusion trimer (Fig. 1F) (4, 7). The hydrophobic fusion loops, buried at the dimer interface in the prefusion structure (3, 5, 6), cluster into a large hydrophobic surface at one end of the postfusion trimer (4, 7, 8). In this orientation, the fusion loops attach the virus to the target cell membrane. The membrane-proximal stem has two predicted amphipathic helices that lie half-buried in the outer leaflet of the viral membrane (Fig. 1C) (9, 10). For fusion to take place, this stem must span the length of domain II (Fig. 1F). A likely model is that it "zips up" along the gaps between the clustered domains, bringing together the transmembrane anchor and the fusion loops, inducing deformation of their associated membranes and leading to membrane merger.

Several studies show the importance of the amino-terminal part of the stem and suggest that it forms contacts with domain II as the fusion-inducing transition proceeds (11–13). Efforts to visualize it directly in this conformation have failed, however, because including the stem residues in recombinant E generally leads to instability or aggregation of any secreted product. We describe here a method for producing sE that includes portions of the juxtamembrane stem and report its crystallization and structure determination. The structure shows that the N-terminal part of the stem zips up along the seam between adjacent domains II in the trimer. The rest of the stem in our constructs is disordered. The arrangement of the trimer core is the same as in previous, stemless structures. The results are consistent with a model in which the N-terminal (proximal) stem stabilizes a trimer with clustered fusion loops, while the central part (residues 404 to 421) has few, if any, contacts with the folded domains in the E trimer.

MATERIALS AND METHODS

Expression, purification, and crystallization. Dengue virus serotype 1 (DV1) Western Pacific 74 (WP-74) sE was cloned from cDNA of a laboratory strain of infectious virus. The cDNA was generated by viral RNA extraction using QIAamp (Qiagen) followed by reverse transcriptase PCR (RT-PCR) using Superscript III (Invitrogen). The E protein sequence was subcloned into a pFastbac plasmid for expression in *Trichoplusia ni* cells. The E sequence followed a signal peptide from human Wnt 3 and an octa-His tag. The mature N terminus has the sequence GHHHHHHHH GSSTSNG prior to the initial residue of E. The fusion loop tryptophan was mutated to histidine to increase solubility (W101H). We produced two constructs, one ending at residue 411 and a longer one ending at residue 421. The shorter construct, sE(1-411), has the sequence EK at positions 202 and 203; the longer construct, sE(1-421), has KE. These positions are in a loop that is not involved in any contacts and probably reflect differences in the laboratory virus population. Both sequences can be found in FLAVIdb (14).

The protein was purified essentially as described in references 15 and 16. *Trichoplusia ni* cells were grown in Ex-Cell405 (Sigma-Aldrich) medium and infected at 1 million/ml. Supernatant was clarified 72 h after infection by centrifugation and passed twice over cobalt resin (Clontech). The resin was washed with 10 mM imidazole in Dulbecco's modified phosphate-buffered saline (Sigma-Aldrich) and eluted in the same buffer with 200 mM imidazole. The protein was concentrated in a Centricon 30kd spin concentrator (Millipore) and then passed over a Superdex 200 10/300 GL size exclusion chromatography column (GE Healthcare Life Sciences) in 20 mM triethanolamine buffer, pH 8.0, with 150 mM NaCl. The protein was concentrated to 10 to 15 mg/ml for crystallization trials. Crystals were grown at 20°C by hanging-drop vapor diffusion by mixing 0.6 μl each of protein and reservoir solution (15 to 20% polyethylene glycol 400 [PEG 400], 0.1 M sodium acetate [pH 4.5], 0.1 M $CdCl_2$). Hexagonal

Received 7 November 2012 **Accepted** 4 December 2012
Published ahead of print 12 December 2012
Address correspondence to Stephen C. Harrison, harrison@crystal.harvard.edu.

doi:10.1128/JVI.02957-12

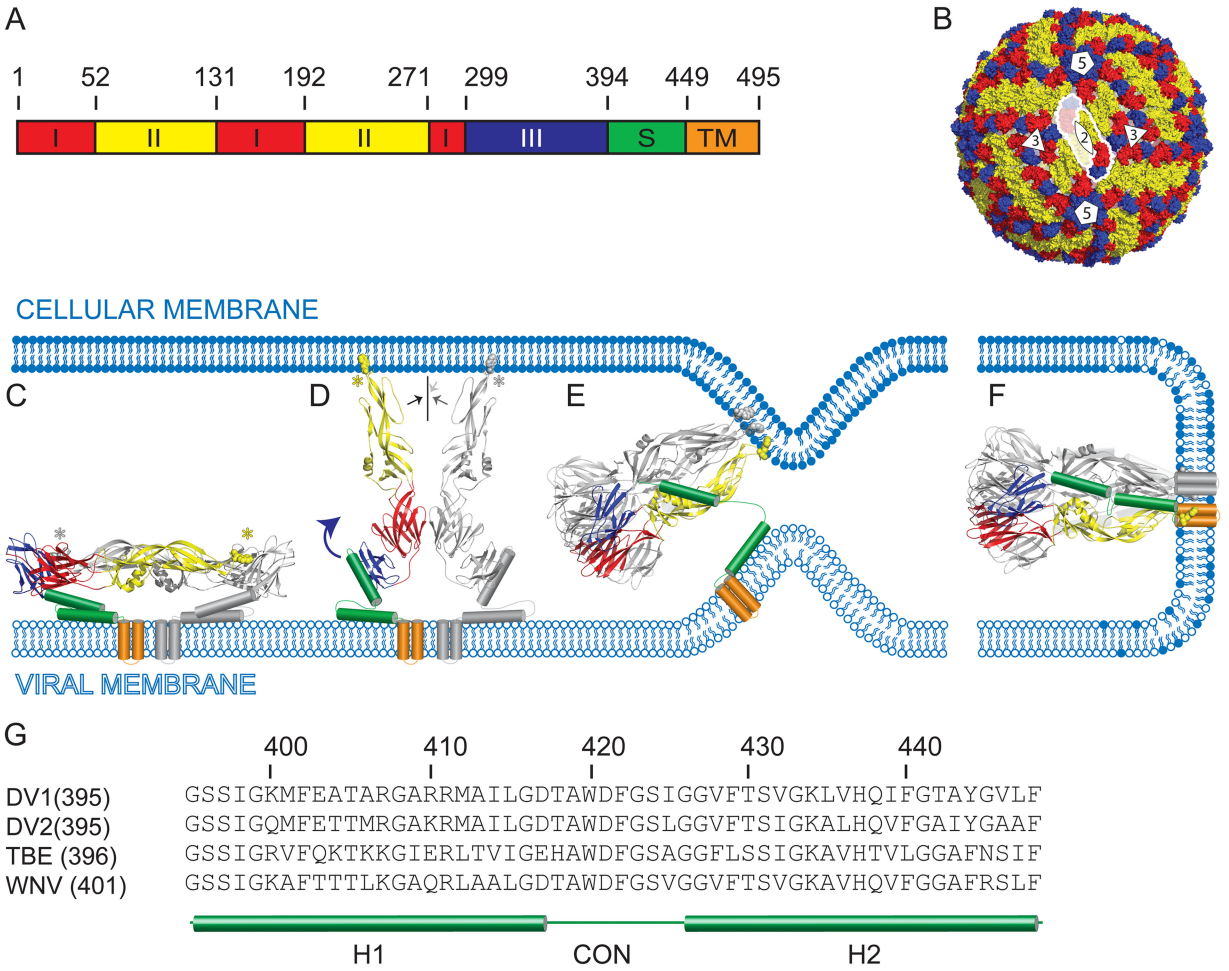

FIG 1 The dengue virus E protein. (A) Linear representation, showing distribution of the polypeptide chain among three domains I to III, colored red, yellow, and blue, respectively. Domain III leads into a juxtamembrane stem (S) region (green), which links the extracellular region to a carboxy-terminal double-pass transmembrane anchor (TM). (B) Packing of E on the surface of a mature virion. Ninety E dimers are arranged on an icosahedral lattice (10). Symmetry operators are shown in white. Monomers at the center 2-fold axis are outlined with a white line, with a single monomer faded for clarity. (C to F) The fusion process schematized. (C) The dimer lies flat on the viral membrane in the mature prefusion state, with the fusion loops (asterisks) buried in dimer contacts. The two predicted amphipathic helices (green) of the stem lie against the membrane. (D) Low pH causes the dimer to dissociate and the monomers to project outward; the fusion loops are shown buried in the target cell membrane. Domain III folds back and rebinds on the side of domain I, stabilizing a trimer. The arrows indicate that the angle between domains I and II changes, allowing the fusion loops of the three copies of domain II to come together. (E) The stem extends along the seam between two domains II, but the distal stem and membrane anchor are not yet in contact with the fusion loop. (F) All three stems traverse the entire length of domain II, bringing together the TM anchor and the fusion loop, completing membrane merger and pore formation. (G) Amino acid sequence of the stem. Between the two predicted amphipathic helices (H1 and H2) is a conserved region (CON), which varies little across all flaviviruses. The stem sequences of DV1 and DV2 are aligned with those of TBE and West Nile virus (WNV).

plates grew in hours and reached maximal size in several days. Diffraction data were collected at the Advanced Photon Source (APS) at Argonne National Laboratories and the Advanced Light Source (ALS) at Lawrence Berkeley National Laboratories (see Table 1 for statistics). Data were integrated and scaled with HKL2000 (17).

Structure determination. The initial structure of sE(1-411) was determined by molecular replacement with the published DV1 sE structure (Protein Data Bank code: 3G7T), using the program suite Phaser (8, 18). The crystals were originally scaled in $P6_322$, the same space group as the structure of stemless DV1 sE (8), but refinement in this space group failed. Refinement of the structure was possible when scaled in $P6_3$ with a significant twin fraction (h,−h−k,−l). Refinement was carried out with Phenix using rigid body and TLS groups (19). Building and rebuilding were carried out in iterative cycles using the 2Fo-Fc and Fo-Fc Fourier maps in COOT (20). The refined structure of DV1 sE(1-411) was used for the molecular replacement of sE(1-421). sE(1-421) was then refined using Phenix to optimize X-ray and stereochemistry weight.

In both molecules of the asymmetric unit, the model includes residues 2 to 403, omitting one disordered segment (D147 to E157). The fusion loop W101H of molecule B could not be placed unambiguously, and there was inadequate density for the side chains of several residues in molecule B (E84, H244, K246, K247, K343, E362, and K385). The first *N*-acetyl-D-glucosamine (NAG) was modeled on N67 of both molecules. The other predicted glycosylation, N153, is in the disordered loop. Four Cd ions and one Cl ion were also placed in both structures. Interface calculations were carried out with PDBePISA (Protein Interfaces, Surfaces and Assemblies) at the European Bioinformatics Institute (http://www.ebi.ac.uk/pdbe/prot_int/pistart.html) (21). Figures were created using the PyMOL molecular graphics system (Schrödinger, LLC).

Protein structure accession numbers. The atomic coordinates and structure factors of DV1 sE(1-411) and sE(1-421) have been deposited in

TABLE 1 Data collection and refinement statistics[a]

Parameter	sE(1–411)	sE(1–421)
Data collection	APS (24IDE)	ALS (8.2.2)
Wavelength (Å)	0.979	0.999
Space group	$P6_3$	$P6_3$
Cell dimensions		
a, *b*, *c* (Å)	77.57, 77.57, 292.52	77.89, 77.89, 292.29
α, β, γ (°)	90, 90, 120	90, 90, 120
Resolution (Å)	50–1.90 (1.97–1.90)	50–2.57 (2.66–2.57)
R_{merge}	0.104 (0.455)	0.116 (0.521)
$I/\sigma I$	14.2 (1.84)	15.38 (1.92)
Completeness (%)	99.1 (98.3)	99.6 (96.1)
Redundancy	5.4 (5.1)	10.4 (7.3)
Refinement		
Resolution (Å)	26.18–1.90 (1.94–1.90)	28.48–2.57 (2.65–2.57)
No. of reflections work/free	72973/3879 (3534/173)	30182/1562 (2707/135)
Twin law	h,−h−k,−l	h,−h−k,−1
Twin fraction	0.4	0.5
R_{work}/R_{free}	0.161/0.186 (0.246/0.267)	0.176/0.209 (0.252/0.344)
Model (atoms)		
Protein	5944	5944
NAG	28	28
Cd	4	4
Cl	1	1
Water	666	223
B avg (Å^2)	19.93	15.67
RMSD		
Bond length (Å)	0.012	0.003
Bond angle (°)	1.29	0.642
Ramachandran (%)		
Favored	96.4	95.6
Allowed	3	4
Outliers	0.6	0.4

[a] Values for the highest-resolution shell are shown in parentheses. R_{merge}, $\Sigma_{h,k,l}\Sigma_i|I_i(hkl) - <I(hkl)>|/\Sigma_{h,k,l}\Sigma_i I_i(hkl)$, where *I* is an intensity that is observed *i* times; $I/\sigma I$, signal-to-noise ratio (average observed intensity divided by average standard deviation of the observed intensity); R_{work}, $\Sigma_{h,k,l}||F_{obs}| - |F_{calc}||/\Sigma_{h,k,l}|F_{obs}|$, where *h*, *k*, *l* covers the "working set" of observed structure factor amplitude (F_{obs}) reflections used in refinement (all reflections minus the test set) and F_{calc} is the calculated structure factor amplitude; R_{free}, calculated as for R_{work} but on 5% of data excluded before refinement.

the Protein Data Bank with accession numbers 4GSX and 4GT0, respectively.

RESULTS

Expression of sE with parts of the stem. Previous structural studies of sE used protein obtained either from limited trypsin digestion of virions or from stable insect cell lines (3, 6). To screen constructs rapidly, we expressed sE in Hi5 insect cells, using a baculovirus vector. We could derive milligram quantities of stemless sE from baculovirus-infected insect cells without needing to coexpress the prM chaperone protein (3).

Initial attempts to secrete sE containing various lengths of contiguous stem failed to produce sufficient quantities of protein, probably because stem hydrophobicity caused endoplasmic reticulum (ER) retention (9). To increase yields, we placed the His tag at the amino terminus immediately after the signal peptide, where it disrupts dimer formation and decreases the potential for hydrophobic aggregation. We also mutated Trp101 in the fusion loop to His (W101H), so that the loop would be charged under the low pH of insect cell expression media. These mutations allowed us to obtain high yields of secreted, monomeric DV1 sE with partial stem appended and to purify the protein from the insect cell medium.

Crystallization of trimeric sE. Trimerization of sE *in vitro* generally requires membrane association to overcome a high kinetic barrier, and the very stable trimers can then be purified in the presence of detergents. The fusion loop mutation (W101H) we introduced for expression prevents membrane insertion. We therefore screened low-pH crystallization conditions to capture the postfusion trimer form in the absence of detergents, as described recently by Nayak and colleagues (8).

Two different forms of extended sE—sE(1-411) and sE(1-421)—crystallized readily as hexagonal plates at pH 4.5 in the presence of 0.1 M $CdCl_2$. sE(1-411) contains most of the predicted amphipathic helix 1 (H1) (Fig. 1); sE(1-421) contains the entire H1 and half of the conserved region between the two putative helices. We recorded diffraction from crystals of sE(1-411) to Bragg spacings smaller than 2 Å. Crystals of both variants had identical packing, with a root mean square deviation (RMSD) of 0.25 Å for all protein atoms. There are two molecules in the asymmetric unit of the twinned $P6_3$ structures. The two molecules have a main-chain RMSD of 0.79 Å. Molecule A of both structures is more complete and has slightly better density and was therefore used for the following analysis and comparisons.

Stem interactions. The structurally defined part of the stem (residues 395 to 403) extends along the seam between adjacent molecules in the trimer (Fig. 2). The interaction buries more than 60% of the stem surface, evenly split between the two neighboring subunits. The stem interactions alternate between protomers along the seam, effectively zippering adjacent molecules together. G399, M401, and E403 of the stem interact with the h-i loop of the adjacent molecule, disordered in the previously published, stemless DV1 structure. The amino acid sequence in the h-i loop is not well conserved among flaviviruses, perhaps because many of the observed loop interactions are main-chain contacts and hence less sensitive to residue identity. Certain hydrophobic side chains are critical, however. The side chain of I398 fills a hole between two protomers, and M401 is buried under the h-i loop. I398 is strictly conserved, and residue 401 is always hydrophobic (Fig. 1G). A key hydrophobic interaction involves the strictly conserved F402 (Fig. 1G), which packs against a conserved, hydrophobic patch made up of domain II residues L216, P217, L218, and M260 (Fig. 2).

Beyond residue 403, the extended chain of the stem cannot span the gap between adjacent subunits, and the density in the map falls off abruptly. The identities of the succeeding residues also vary among flaviviruses.

Comparison to other dengue virus structures. The structure of the trimer core is very similar to the previously determined, stemless 3.5-Å DV1 sE structure (PDB code: 3G7T), with a main-chain RMSD of 1.46 Å (Fig. 3A). In the stemless DV1 sE trimer, His 27, His 282, His 317, and Glu 368 form a polar cluster, linking together domains I and III (Fig. 3B). The crystals that yielded that structure grew at pH 6.5, close to the histidine pK_a (8). The pH at which our crystals grew (4.5) would ensure protonation of histidines, destabilizing the polar cluster. Indeed, nearly all the cluster contacts are missing (Fig. 3B). In the B molecule, a Cd ion bridges

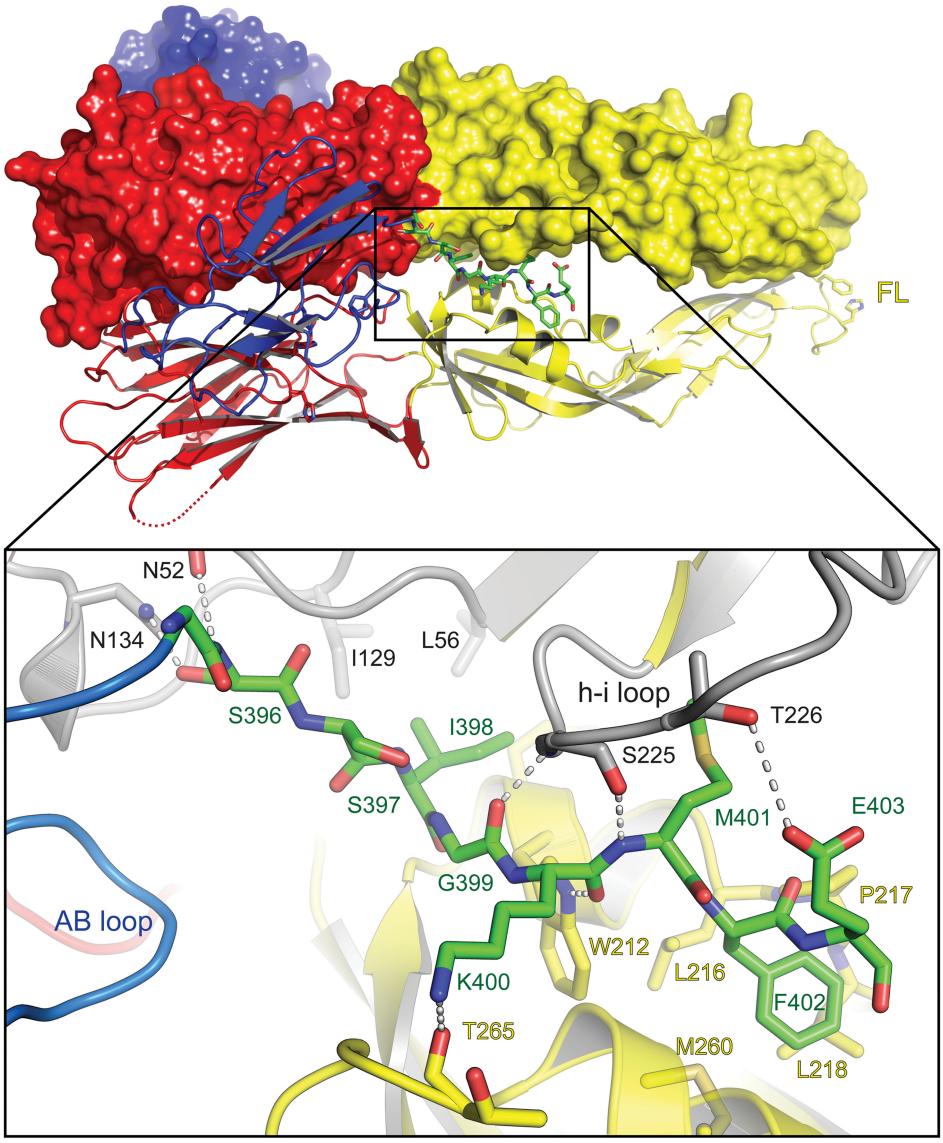

FIG 2 Stem contacts. For clarity, only two monomers of the trimer are shown, with one monomer in surface representation. The orientation is essentially the same as in Fig. 1F. The fusion loop (FL) on the right shows the W101H mutation. The stem is in green. The zoomed inset shows interactions of the stem with the same monomer (color) and the adjacent monomer (gray). Water-bridged hydrogen bonds have been removed. The AB loop of the stem molecule and h-i loop of the adjacent molecule are labeled (designations as in reference 4).

His 27, His 282, and Glu 368, but His 317 and the AB loop are in the same conformation as in the A molecule, shifted away from Glu 368.

In the stemless DV1 structure, the fusion loop phenylalanine, F108, projects toward the center of the 3-fold axis, forming additional trimer contacts (8). It was suggested that either the lack of detergents or long-range effects of unconserved regions might account for the unique conformation. Here, despite nearly identical packing, the fusion loop of molecule A is in the more typical orientation (Fig. 3C): F108 overlays well onto the corresponding residue in the DV2 structure (PDB code: 1OK8), despite the presence of the fusion loop mutation at W101H.

Trimer packing. How does the presence of the stem affect trimer packing? There is a hinge between domains I and II (4, 22, 23); its angle changes by approximately 30° in the transition from the prefusion dimer conformation to the fusion loop clustered trimer conformation (3, 4). If the domain I-II dimer angle is applied to the trimer (by superposing domain I of the dimer structure onto the trimer), each fusion loop is 21 Å farther from the center of the 3-fold axis in the plane of the membrane than in the fusion loop clustered conformation (Fig. 4), producing a trimer with a tripod-like appearance (Fig. 4A). Molecular dynamics simulations at low pH have suggested that trimeric, stemless sE might adopt this open conformation (24). Indeed, a recent stemless flavivirus crystal structure reveals splayed fusion loops at an intermediate distance, 17 Å, from the 3-fold axis, 5 Å farther than in the closed conformation (25). It has also been proposed that during the final stages of fusion, the H1 segment of the stem would squeeze between adjacent domains II, maintaining the splayed conformation (7). The open conformation is not compatible, however, with the

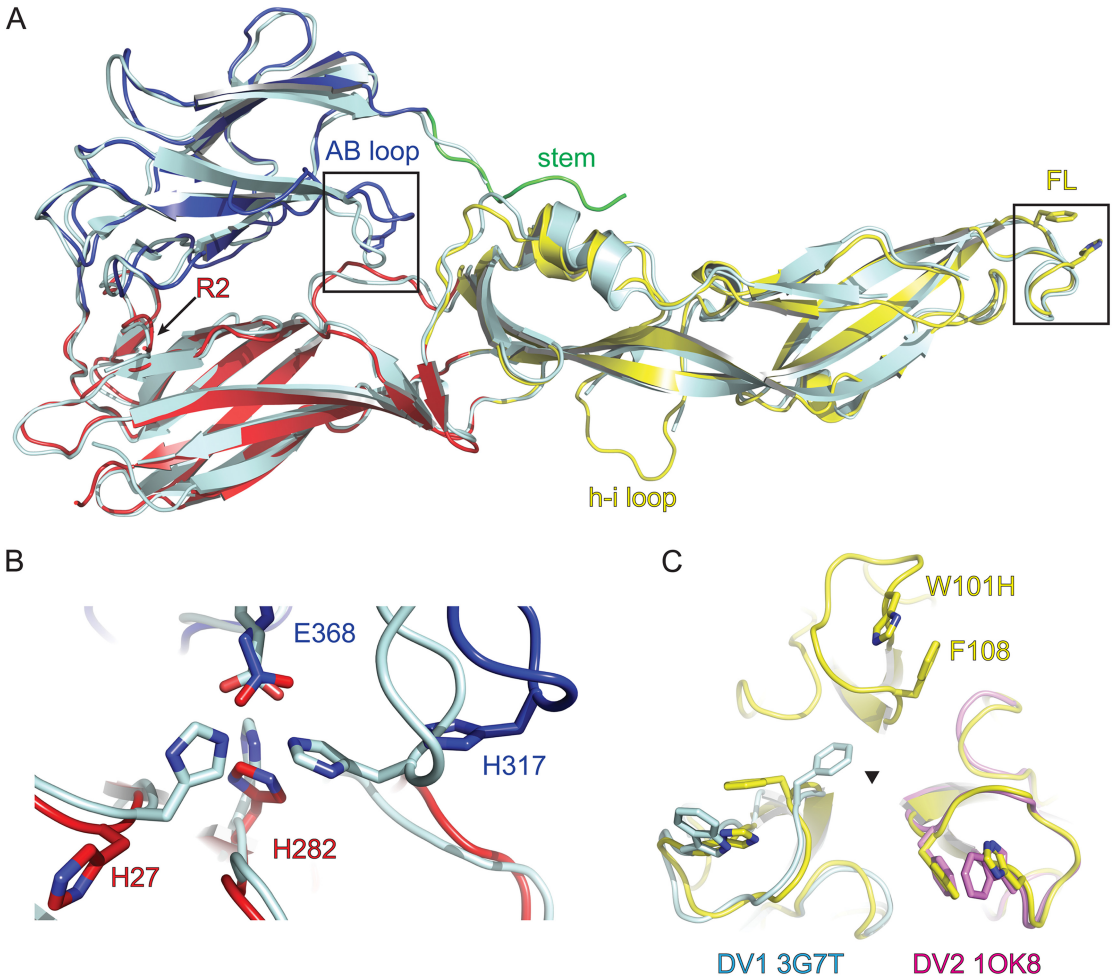

FIG 3 Comparison with other dengue virus E structures. (A) The sE monomer shown is in essentially the same orientation as in Fig. 1F and Fig. 2. DV1 sE is in color. The stemless DV1 trimer (PDB code: 3G7T) is in cyan. The stem and h-i loop are labeled. The most amino-terminal residue of the model (arginine 2) is labeled R2. The principal differences between the two structures are boxed: the AB loop and the fusion loop (FL). (B) The AB loop in the stemless structure participates in a polar cluster linking domains I and III. In the present structure, H317 of the AB loop projects away from the polar cluster. (C) The trimer fusion loops, viewed along the 3-fold axis. The fusion loop W101H mutation and F108 are labeled. Monomers of DV1 sE (PDB code: 3G7T) and DV2 sE (PDB code: 10K8) are superposed on the trimer and shown in cyan and pink, respectively. In the structure described here, F108 adopts the more typical orientation, directed away from the 3-fold axis.

zipped-up stem conformation we observe. A splayed structure (if it indeed ever occurred) could, in principle, be an intermediate between folding back of domain III and reconfiguration of the stem.

DISCUSSION

We report a strategy for expressing flavivirus sE with parts of the juxtamembrane stem and describe the (essentially identical) crystal structures of trimeric DV1 sE with subunits that extend along the stem to positions 411 and 421. In both cases, the proximal stem zips up between adjacent domains II, but the tight interaction continues only to residue 403, and the remaining stem residues in our constructs are disordered. The structure we report is consistent with earlier findings, indicating a role for the proximal stem in enhancing trimer formation and domain III binding (11, 12). It also agrees with more recently reported biochemical studies on tick-borne encephalitis virus (TBE) fusion that implicate F402 in intramolecular contacts with domain II (13). The latter work led to a proposal that F402 might interdigitate between W212 and L216. In the DV1 trimer, F402 indeed has what appear to be important hydrophobic contacts, but instead of packing between W212 and L216, it lies against a conserved hydrophobic surface created by the side chains of L216, L218, and M260. The mutations introduced in the work on TBE could readily have perturbed or remodeled this hydrophobic patch.

The absence of strong contacts that could immobilize residues 404 to 421 is consistent with studies of peptides binding to a stemless sE trimer (26). Stem-derived peptides that cover the distal stem (residues 419 to 440) bind very tightly, whereas peptides that cover the proximal stem (residues 396 to 429) do not. The zipper-like contact we see for residues 396 to 403 is evidently strong enough to immobilize a covalently attached stem segment but not to bind a soluble peptide.

Rearrangements in E required in the transition from prefusion dimer to postfusion trimer, illustrated in Fig. 1C to F, involve the folding back of domain III against domain I and zipping up of the stem along clustered domains II. Stem zipping cannot occur until

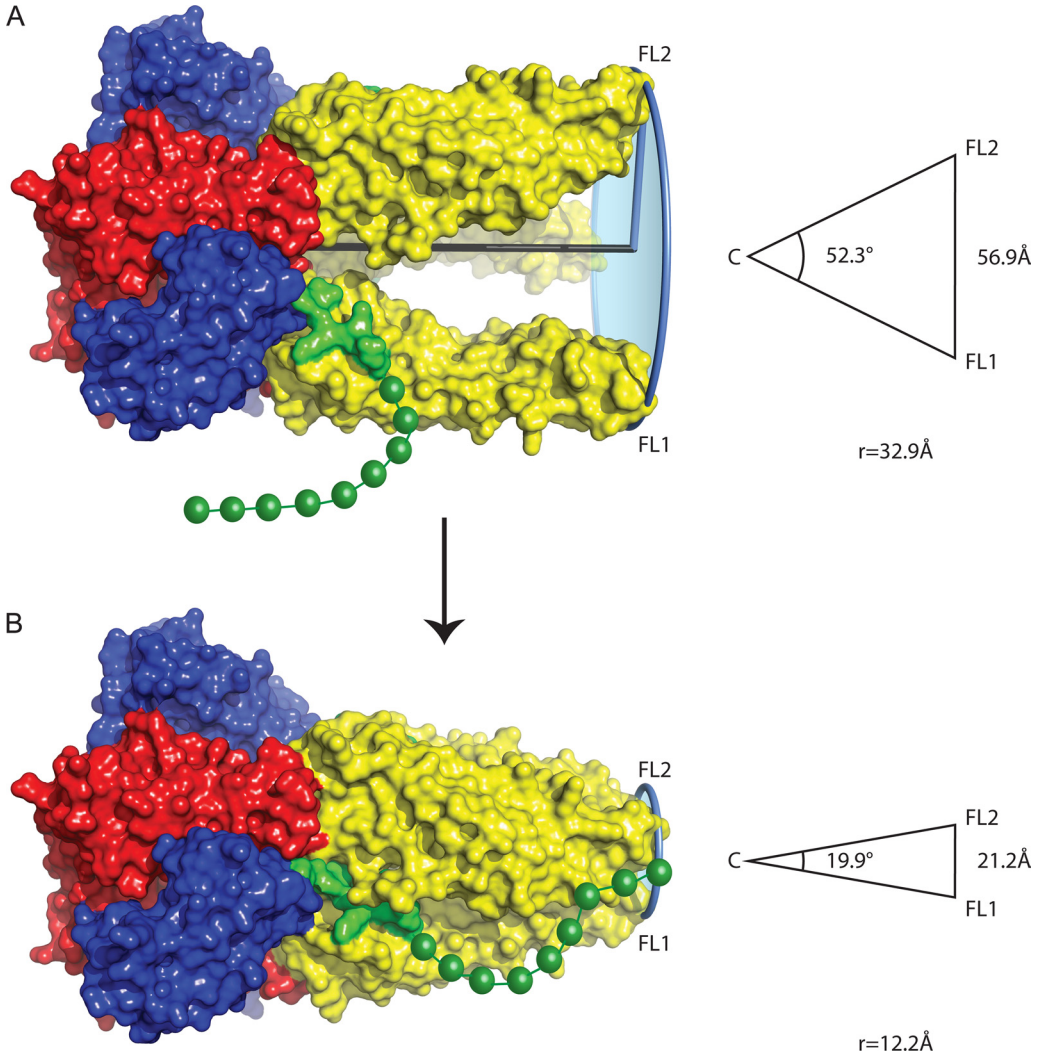

FIG 4 The stem stabilizes a closed trimer conformation. (A) Representation of a hypothetical splayed trimer with the domain I-II hinge in the same orientation as in the DV2 dimer (PDB code: 1OAN). The stem (green) is shown with the intramolecular interactions from Fig. 2: the gap is too great to contact the adjoining molecule. The remainder of the stem, including the disordered residues 404 to 421, is shown as green beads on a string. The angle between 2 fusion loops and the center (C) of the 3-fold axis at the domain I-II junction is 52.3°; the fusion loops are nearly 57 Å apart. The plane of the membrane is shown in light blue bounded by a circle that circumscribes all three fusion loops. The radius (blue rod) (r) defines the distance from the FL to the center of the 3-fold axis (black rod) in the plane of the membrane. (B) In the observed structure, stem contacts bridge between the subunits. The angle is closed by more than 30° compared with the splayed trimer; the fusion loop separation is about 21 Å. The distal part of the stem, including H2, is shown as beads that interact near the fusion loops.

domain III has folded back, and the structure we report probably represents a later-stage intermediate in the course of the fusion-promoting E conformational change than does the stemless sE trimer. This zippering can stabilize a fusion loop clustered trimer (Fig. 4) and drive membrane-coupled conformational collapse. Tight binding of stem peptides (residues 419 to 440) indicates that the most distal stem interactions are probably quite strong (26, 27). A plausible picture for the final, postfusion state of the complete E trimer would then allow residues between 404 and 420 (roughly) to loop out from close contact with the domain II 3-fold cluster and residues of the distal stem to contact the region near the fusion loop tip (Fig. 4B).

ACKNOWLEDGMENTS

We thank members of the Harrison laboratory for comments and suggestions, Aaron Schmidt and Priscilla Yang for providing the dengue serotype 1 cDNA, Simon Jenni for helping with data processing and PyMOL scripts, and the staffs of beamlines at ALS and APS.

This work was supported by NIH grant U54AI057159 (SCH project of the New England Regional Center of Excellence for Biodefense and Emerging Infectious Diseases, D. Kasper, principal investigator). D.E.K. is a Howard Hughes Medical Institute Fellow of the Life Sciences Research Foundation. S.C.H. is an investigator of the Howard Hughes Medical Institute. The Berkeley Center for Structural Biology is supported in part by the National Institutes of Health, National Institute of General Medical Sciences, and the Howard Hughes Medical Institute; the ALS is supported by the Director, Office of Science, Office of Basic Energy Sciences, of the U.S. Department of Energy (DOE) under contract no. DE-AC02-05CH11231. The Northeastern Collaborative Access Team beamlines at APS are supported by grants from the National Center for Research Resources (5P41RR015301-10) and the National Institute of General Medical Sciences (8 P41 GM103403-10) of the National Institutes of Health. Use of the APS, an Office of Science User Facility operated for the U.S.

DOE Office of Science by Argonne National Laboratory, was supported by the U.S. DOE under contract no. DE-AC02-06CH11357.

REFERENCES

1. **Lindenbach BD, Thiel H-J, Rice CM.** 2007. *Flaviviridae*: replication. *In* Knipe DM, Howley PM, Griffin DE, Lamb RA, Martin MA, Roizman B, Straus SE (ed), Fields virology, 5th ed, vol 1. Lippincott Williams & Wilkins, Philadelphia, PA.
2. **Harrison SC.** 2008. Viral membrane fusion. Nat. Struct. Mol. Biol. **15**: 690–698.
3. **Modis Y, Ogata S, Clements D, Harrison SC.** 2003. A ligand-binding pocket in the dengue virus envelope glycoprotein. Proc. Natl. Acad. Sci. U. S. A. **100**:6986–6991.
4. **Modis Y, Ogata S, Clements D, Harrison SC.** 2004. Structure of the dengue virus envelope protein after membrane fusion. Nature **427**:313–319.
5. **Allison SL, Schalich J, Stiasny K, Mandl CW, Heinz FX.** 2001. Mutational evidence for an internal fusion peptide in flavivirus envelope protein E. J. Virol. **75**:4268–4275.
6. **Rey FA, Heinz FX, Mandl C, Kunz C, Harrison SC.** 1995. The envelope glycoprotein from tick-borne encephalitis virus at 2 A resolution. Nature **375**:291–298.
7. **Bressanelli S, Stiasny K, Allison SL, Stura EA, Duquerroy S, Lescar J, Heinz FX, Rey FA.** 2004. Structure of a flavivirus envelope glycoprotein in its low-pH-induced membrane fusion conformation. EMBO J. **23**:728–738.
8. **Nayak V, Dessau M, Kucera K, Anthony K, Ledizet M, Modis Y.** 2009. Crystal structure of dengue virus type 1 envelope protein in the postfusion conformation and its implications for membrane fusion. J. Virol. **83**: 4338–4344.
9. **Stiasny K, Allison SL, Marchler-Bauer A, Kunz C, Heinz FX.** 1996. Structural requirements for low-pH-induced rearrangements in the envelope glycoprotein of tick-borne encephalitis virus. J. Virol. **70**:8142–8147.
10. **Zhang W, Chipman PR, Corver J, Johnson PR, Zhang Y, Mukhopadhyay S, Baker TS, Strauss JH, Rossmann MG, Kuhn RJ.** 2003. Visualization of membrane protein domains by cryo-electron microscopy of dengue virus. Nat. Struct. Biol. **10**:907–912.
11. **Allison SL, Stiasny K, Stadler K, Mandl CW, Heinz FX.** 1999. Mapping of functional elements in the stem-anchor region of tick-borne encephalitis virus envelope protein E. J. Virol. **73**:5605–5612.
12. **Liao M, Kielian M.** 2005. Domain III from class II fusion proteins functions as a dominant-negative inhibitor of virus membrane fusion. J. Cell Biol. **171**:111–120.
13. **Pangerl K, Heinz FX, Stiasny K.** 2011. Mutational analysis of the zippering reaction during flavivirus membrane fusion. J. Virol. **85**:8495–8501.
14. **Olsen LR, Zhang GL, Reinherz EL, Brusic V.** 2011. FLAVIdB: a data mining system for knowledge discovery in flaviviruses with direct applications in immunology and vaccinology. Immunome Res. **7**:1–9.
15. **Klein DE, Nappi VM, Reeves GT, Shvartsman SY, Lemmon MA.** 2004. Argos inhibits epidermal growth factor receptor signalling by ligand sequestration. Nature **430**:1040–1044.
16. **Klein DE, Stayrook SE, Shi F, Narayan K, Lemmon MA.** 2008. Structural basis for EGFR ligand sequestration by Argos. Nature **453**:1271–1275.
17. **Otwinowski Z, Minor W.** 1997. Processing of X-ray diffraction data collected in oscillation mode. Methods Enzymol. **276**:307–326.
18. **McCoy AJ, Grosse-Kunstleve RW, Adams PD, Winn MD, Storoni LC, Read RJ.** 2007. Phaser crystallographic software. J. Appl. Crystallogr. **40**: 658–674.
19. **Adams PD, Afonine PV, Bunkoczi G, Chen VB, Davis IW, Echols N, Headd JJ, Hung LW, Kapral GJ, Grosse-Kunstleve RW, McCoy AJ, Moriarty NW, Oeffner R, Read RJ, Richardson DC, Richardson JS, Terwilliger TC, Zwart PH.** 2010. PHENIX: a comprehensive Python-based system for macromolecular structure solution. Acta Crystallogr. D Biol. Crystallogr. **66**:213–221.
20. **Emsley P, Lohkamp B, Scott WG, Cowtan K.** 2010. Features and development of Coot. Acta Crystallogr. D Biol. Crystallogr. **66**:486–501.
21. **Krissinel E, Henrick K.** 2007. Inference of macromolecular assemblies from crystalline state. J. Mol. Biol. **372**:774–797.
22. **Kanai R, Kar K, Anthony K, Gould LH, Ledizet M, Fikrig E, Marasco WA, Koski RA, Modis Y.** 2006. Crystal structure of West Nile virus envelope glycoprotein reveals viral surface epitopes. J. Virol. **80**:11000–11008.
23. **Nybakken GE, Nelson CA, Chen BR, Diamond MS, Fremont DH.** 2006. Crystal structure of the West Nile virus envelope glycoprotein. J. Virol. **80**:11467–11474.
24. **Dubey KD, Chaubey AK, Ojha RP.** 2012. Stability of trimeric DENV envelope protein at low and neutral pH: an insight from MD study. Biochim. Biophys. Acta **1834**:53–64.
25. **Luca VC, Nelson CA, Fremont DH.** 2012. Structure of the St. Louis encephalitis virus postfusion envelope trimer. J. Virol. doi:10.1128/JVI.01950-12.
26. **Schmidt AG, Yang PL, Harrison SC.** 2010. Peptide inhibitors of dengue-virus entry target a late-stage fusion intermediate. PLoS Pathog. **6**:e1000851. doi:10.1371/journal.ppat.1000851.
27. **Schmidt AG, Yang PL, Harrison SC.** 2010. Peptide inhibitors of flavivirus entry derived from the E protein stem. J. Virol. **84**:12549–12554.